

# Metastable Dark Energy with Radioactive-like Decay

Arman Shafieloo,<sup>1,2\*</sup> Dhiraj Kumar Hazra,<sup>3</sup> Varun Sahni<sup>4</sup> and Alexei A. Starobinsky<sup>5,6</sup>

<sup>1</sup>*Korea Astronomy and Space Science Institute, Daejeon 34055, Korea*

<sup>2</sup>*University of Science and Technology, Daejeon 34113, Korea*

<sup>3</sup>*AstroParticule et Cosmologie (APC)/Paris Centre for Cosmological Physics, Université Paris Diderot, CNRS, CEA, Observatoire de Paris, Sorbonne Paris Cité University, 10, rue Alice Domon et Leonie Duquet, 75205 Paris Cedex 13, France*

<sup>4</sup>*Inter-University Centre for Astronomy and Astrophysics, Post Bag 4, Ganeshkhind, Pune 411 007, India*

<sup>5</sup>*Landau Institute for Theoretical Physics RAS, Moscow, 119334, Russia*

<sup>6</sup>*Bogolyubov Laboratory of Theoretical Physics, Joint Institute for Nuclear Research, Dubna 141980, Russia*

Accepted XXX. Received YYY; in original form ZZZ

## ABSTRACT

We propose a new class of metastable dark energy (DE) phenomenological models in which the DE decay rate does not depend on external parameters such as the scale factor or the curvature of the Universe. Instead, the DE decay rate is assumed to be a constant depending only on intrinsic properties of DE and the type of a decay channel, similar to case of the radioactive decay of unstable particles and nuclei. As a consequence, the DE energy density becomes a function of the proper time elapsed since its formation, presumably in the very early Universe. Such a natural type of DE decay can profoundly affect the expansion history of the Universe and its age. Metastable DE can decay in three distinct ways: (i) exponentially, (ii) into dark matter, (iii) into dark radiation. Testing metastable DE models with observational data we find that the decay half-life must be many times larger than the age of the Universe. Models in which dark energy decays into dark matter lead to lower values of the Hubble parameter at large redshifts relative to  $\Lambda$ CDM. Consequently these models provide a better fit to cosmological BAO data (especially data from high redshift quasars) than concordance ( $\Lambda$ CDM) cosmology.

**Key words:** Observational Cosmology – Dark Energy –

## 1 INTRODUCTION

One of the main goals of physical cosmology is to understand the nature of the constituents of our Universe. Of these perhaps the most enigmatic are dark matter and dark energy (DE) which, together, constitute nearly 96% of the total density of the Universe (Sahni & Starobinsky 2000; Sahni 2004). While many theoretical models have been advanced to explain the nature of the dark Universe, what has firmly been established is that dark matter clusters and has a pressureless equation of state, while dark energy possesses negative pressure which can cause the Universe to accelerate (Carroll 2001; Peebles & Ratra 2003; Padmanabhan 2003; Sahni 2005; Copeland et al. 2006; Sahni & Starobinsky 2006). It is also widely believed that both dark matter and dark energy have a non-baryonic origin. The current debate on the nature of the dark Universe allows for the fact that the two dark components might interact with each other. The transfer of energy between dark energy and dark matter could lead to interesting, and possibly unique, observational sig-

natures; see (Amendola 2000; Guo et al. 2007; Boehmer et al. 2008; Valiviita et al. 2008; He & Wang 2008; Micheletti et al. 2009; He et al. 2011; Pavan et al. 2012; Faraoni et al. 2014; Salvatelli et al. 2014; Ferreira et al. 2017) and references therein.

Existing observational data do not show any statistically significant deviation from concordance cosmology in which DE coincides with an exact cosmological constant  $\Lambda$  and is therefore stable and eternal. However, the remarkable *qualitative* similarity between the physical properties of current DE and the primordial DE that drove inflation in the very early Universe (the latter without a doubt being metastable) makes it rather natural (though not obligatory) to put forward the hypothesis that the present DE is metastable and not eternal, too<sup>1</sup>. Historically, such a hypothesis was first advanced in a very old paper by the Soviet

<sup>1</sup> Here we call DE *any* driving force for an accelerated expansion of the Universe, irrespective of its nature. Using the terminology introduced in (Sahni & Starobinsky 2006), DE can be physical (a new field of matter) or geometrical (modified gravity), but most generally it is mixed one like in the case of scalar-tensor gravity.

\* E-mail: shafieloo@kasi.re.kr

physicist Matvei Bronstein in 1933 (Bronstein 1933)<sup>2</sup>. More realistic models of DE which differed from an exact  $\Lambda$ -term began to appear in the 1980's and there are plenty of them by now.

However, in most of these models beginning from (Ozer & Taha 1986), the DE energy density was assumed to be determined by physical properties external to DE itself, for instance DE could depend upon the scale factor of the Friedmann-Lemaitre-Robertson-Walker (FLRW) universe  $a(t)$ , its expansion rate  $H(t)$ , scalar curvature  $R$ , etc.<sup>3</sup> On the other hand, unstable nuclei and elementary particles decay exponentially with time with decay rates not depending on external conditions but defined by their intrinsic composition and structure only. This simple and observed manner of decay has attracted somewhat little attention in studies of the possible decay of DE. In particular, one can hardly find a lower limit on the (decay channel dependent) DE half-life in handbooks, in contrast for instance, to the same quantity for the proton. That is why this paper is devoted to the study of this problem for several models (channels) of DE decay. Using this nuclear physics analogy, we shall call all channels of DE decay in which the decay rate is a constant not depending on space-time metric and curvature radioactive-like ones. We assume that DE decays totally (or almost totally) into other dark (i.e. not participating in strong, electromagnetic and weak interactions) constituents, since the decay of DE into visible matter is strongly restricted by observations. Note that our model of metastable DE closely resembles the decay of dark matter in models in which the latter is composed of metastable particles such as a sterile neutrino. It is well known that a sterile neutrino can decay through the mixing with virtual ("off mass shell") neutrinos and there are even reports that such a decay may be responsible for the emission line at 3.52 keV in the x-ray spectra of the Andromeda galaxy and the Perseus galaxy cluster (Boyarsky et al. 2014).

It follows from the assumption that the DE decay rate is a constant and depends only on its internal composition (in particular, it does not depend on the DE energy density  $\rho_{DE}$ ) that  $\rho_{DE}$  should be a function of the proper time elapsed since the formation of DE (which we assume occurred in the early Universe). Here it is important to emphasize that the energy-momentum tensor of both decaying DE and its decay products should be taken into account in the FLRW equations for  $a(t)$  to avoid inconsistency with the Bianchi identities<sup>4</sup>. Thus, the equation of state  $w \equiv p/\rho$  of the total mixture of DE and its decay products may not be  $w_{tot} = -1$  as is the case for  $\Lambda$ . In fact,  $w_{tot} > -1$ . This allows one to

find a system of reference where this mixture is at rest on the average, and the time in terms of which the DE half-life time is measured is the proper time in this system. We assume that this system is at rest in the FLRW frame, so this time is the usual cosmic time  $t$ .<sup>5</sup>

This 'dark mixture' can be described either totally as one component, or as a sum of two interacting components. In the first case, if some time dependence of  $\rho_{DE}(t)$  is assumed (we keep the name and index 'DE' for this mixture for simplicity and consider the exponential law in the first approximation), the pressure  $p_{DE}$  is defined from the conservation equation as

$$p_{DE} = -\frac{\dot{\rho}_{DE} + 3H\rho_{DE}}{3H} = -\rho_{DE} \left(1 - \frac{\Gamma}{3H}\right) \quad (1)$$

where  $H \equiv \dot{a}/a$  is the Hubble parameter and  $\Gamma = \text{const}$  is the decay rate. This is our model I. In the second case, we may put  $w_1 \equiv w_{DE} = -1$  in the first approximation, and the products of its decay are modeled by either dust-like dark matter with  $w_2 = 0$  (model II) or by dark radiation with  $w_3 = 1/3$  (Model III). Since the aim of the paper is to confront three purely phenomenological ways of DE decay with observational data, we don't set a goal to construct microphysical models producing exactly the same behavior of  $\rho_{DE}(t)$  here. Still in the case of the Model I, a similar behavior naturally occurs in the case of slow rolling quintessence, i.e. if DE is modeled by a minimally coupled scalar field with a sufficiently flat potential, and we discuss it in more details in the Appendix.

In section 2 we discuss these models, while in section 3 we compare their properties against observations and constrain their free parameters. Our results are presented in section 4 and conclusions are drawn in section 5. Broadly speaking our analysis shows that if dark energy is metastable then its decay 'half-life' should exceed the age of the Universe. We find that the decay of dark energy into dark matter alleviates much of the tension faced by concordance cosmology ( $\Lambda$ CDM) when simultaneously fitting CMB data and BAO data from high redshift quasars.

In the Appendix, explicit expressions for the Hubble factor behaviour as a function of redshift are presented in the limit  $\Gamma \ll H_0$ .

## 2 FORMALISM

In this paper we consider three models of metastable dark energy (DE). In Model I, DE decays exponentially and hence has an evolving effective equation of state (EOS). In Model II, DE decays into dark matter, while in Model III, DE decays into dark radiation. We assume that the decay of DE is due to its *intrinsic properties* and is not related to the expansion of the Universe. In particular it could also occur in flat space-time with  $H = 0$ . For simplicity we assume

<sup>2</sup> Since this was shortly before the understanding of the structure of atomic nuclei and the existence of strong interactions, Bronstein tried to use the instability of  $\Lambda$  as a source for the energy of starlight. Still his estimate of the decay rate, considered simply as a (unjustified) hypothesis, was  $\dot{\Lambda}/\Lambda \sim 10^{-24} \text{ s}^{-1}$ , which is so much smaller than the inverse of the present age of the Universe that it cannot be excluded by existing observational data.

<sup>3</sup> The  $\Lambda(H)$  cosmological model (Shapiro & Sola 2002) and its recent "decaying vacuum" extensions such as (Lima et al. 2013) also belong to this class.

<sup>4</sup> It is interesting that a similar critical remark had been immediately made to M. Bronstein by L. Landau, and this was mentioned in the 'Note added' to the paper (Bronstein 1933)

<sup>5</sup> In the presence of isocurvature fluctuations, it is possible that this system has some velocity with respect to the FLRW one, and then part of the CMB temperature dipole is primordial. However, in the absence of extreme fine-tuning, this velocity is non-relativistic and small, so we may neglect it for our purpose.

that DE has the equation of state  $w = -1$  at high redshift, although the methods developed in our paper can easily be generalised to other DE models.

### 2.1 Model I : Exponentially decaying DE

We assume a ‘radioactive decay’ scheme for the time-evolution of dark energy. In other words, the present value of the DE density,  $\rho_{DE}(t_0)$ , is related to its value at an earlier time,  $\rho_{DE}(t)$ , by

$$\rho_{DE}(t) = \rho_{DE}(t_0) \times \exp[-\Gamma(t - t_0)], \quad (2)$$

here, the  $\Gamma$  is the only free parameter in the equation. Eqn (2) follows from

$$\dot{\rho}_{DE} = -\Gamma\rho_{DE}. \quad (3)$$

From (2) one finds the decay ‘half life’ of DE to be  $t_{1/2} = \ln(2)/\Gamma$ , when  $\Gamma > 0$ . Negative values of  $\Gamma$  imply an increase in the DE density with time which corresponds to phantom-like behaviour. Note that  $\Gamma$  has the dimensions of inverse time.

The Hubble parameter,  $h(z) = H(z)/H_0$ , is easily obtained from the FRW equation to be

$$h^2(z) = (1 - \Omega_{0m}) \exp \left[ \frac{\Gamma}{H_0} \int_0^z \frac{dz}{(1+z)h(z)} \right] + \Omega_{0m}(1+z)^3. \quad (4)$$

In what follows we shall solve this equation iteratively to determine the expansion history of the Universe. Note that DE can be described by the dimensionless free parameter  $\Gamma/H_0$ . Hence the decay rate (or growth rate) of DE can be described without knowing the value of  $H_0$ . This is significant since supernovae (SNe) data can directly constrain the decay constant  $\Gamma/H_0$ , thereby describing the half-life of dark energy in units of the age of the Universe.

It is seen from Eq. (1) that the phenomenological decay law (2.1) does not correspond to a constant equation of state  $w_{DE}$ . Moreover,  $w_{DE}$  exceeds unity for  $H < \Gamma/6$ . This shows that this law, if taken literally for all times, might require a rather unusual microscopic model. However, first, we shall use it around the present time only, when  $\Gamma < H_0$  and probably  $\Gamma \ll H_0$ , so that the fraction of already decayed DE is small. Second,  $w_{DE} > 1$  is not prohibited by causality. E.g., it can be easily realized by a usual scalar field with a negative potential minimally coupled to gravity. Thus, because of the ubiquitous appearance of this law in atomic and particle physics, it makes sense to confront it with observations in the case of decaying DE.

### 2.2 Model II: Dark Energy decays into Dark Matter

The basic equations for a model in which DE decays into dark matter are

$$\dot{\rho}_{DE} = -\Gamma\rho_{DE} \quad (5)$$

$$\dot{\rho}_{DM} + 3H\rho_{DM} = \Gamma\rho_{DE} \quad (6)$$

$$\frac{3H^2}{8\pi G} = \rho_{DE} + \rho_{DM} + \frac{3H_0^2}{8\pi G}\Omega_{0b}(1+z)^3. \quad (7)$$

where we have assumed that DE, prior to its decay, had the form of a cosmological constant with  $w = -1$ . This model formally belongs to the class of interacting DM-DE models

considered in many papers, see (Amendola 2000; Guo et al. 2007; Boehmer et al. 2008; Valiviita et al. 2008; He & Wang 2008; Micheletti et al. 2009; He et al. 2011; Pavan et al. 2012; Faraoni et al. 2014; Salvatelli et al. 2014; Ferreira et al. 2017) and the recent review (Wang et al. 2016). However, in almost all of these papers the parameter  $\Gamma$  was assumed to be proportional to  $H$  or some other time dependent variable whereas we assume  $\Gamma$  to be a fundamental constant. For  $\Gamma > 0$  energy flows from the cosmological constant into dark matter (not baryons). It therefore follows that the current value of  $\Omega_{0m}$ , when extrapolated to high redshifts via  $\Omega_{0m}(1+z)^3$  would be higher than the actual total matter density at high  $z$ . This would imply that the expansion rate at high  $z$  was *lower* than that in  $\Lambda$ CDM thereby alleviating some of the tension which exists between concordance cosmology and the lower value of  $H(z = 2.34)$  obtained from quasar-based BAO data (Delubac et al. 2015).

### 2.3 Model III: Dark Energy decays into Dark Radiation

For completeness we also consider a model in which DE decays into ultra-relativistic ‘dark’ particles:

$$\dot{\rho}_{DE} = -\Gamma\rho_{DE} \quad (8)$$

$$\dot{\rho}_{DR} + 4H\rho_{DR} = \Gamma\rho_{DE} \quad (9)$$

$$\frac{3H^2}{8\pi G} = \rho_{DE} + \rho_{DR} + \frac{3H_0^2}{8\pi G}\Omega_{0m}(1+z)^3. \quad (10)$$

Here the non-relativistic matter component includes both dark matter and baryons, and we have neglected the CMB density  $\rho_r$  assuming it to be smaller than that of dark radiation  $\rho_{DR}$  (this is plausible for  $z \lesssim 10$ ).

## 3 ANALYSIS

In order to constrain our three models we use combinations of different cosmological data sets, including:

(i) Supernovae Type Ia data from the Union-2.1 compilation containing 580 Supernovae (Suzuki et al. 2012) within  $z \sim 0.015 - 1.4$ . We use the complete covariance matrix which takes into account systematic effects.

(ii) Four BAO datasets: SDSS DR7 ( $z = 0.35$ ) (Percival et al. 2010), BOSS DR9 ( $z = 0.57$ ) (Anderson et al. 2013), 6DF ( $z = 0.106$ ) (Beutler et al. 2011) and SDSS DR11 BAO measurements of  $H(z)$  data at  $z = 2.34$  (Delubac et al. 2015).

For SDSS DR7 and BOSS DR9 we calculate  $D_V(z)/r_s(z_{\text{drag}})$ <sup>6</sup>. We do not use the BAO data from WiggleZ because the acoustic parameter  $A(z)$  is estimated using a specific shape of the power spectrum. The WiggleZ data may therefore be biased towards a particular form of the primordial power spectrum and using it could bias our overall results.

<sup>6</sup>  $r_s(z_{\text{drag}})$  is the comoving sound horizon at redshift  $z_{\text{drag}}$ , when baryons decouple from photons.  $D_V = [(1+z)^2 D_A^2(z) c z / H(z)]^{1/3}$  where  $D_A$  is the angular diameter distance.

(iii) We include the CMB into our analysis by using the CMB shift parameters  $R, l_a$  together with the baryon density  $\Omega_{\text{b}}h^2$ . The shift parameters are defined as follows:  $R = \sqrt{\Omega_{\text{m}}H_0^2}r(z_*)/c$  and  $l_a = \pi r(z_*)/r_s(z_*)$ ,  $r(z_*)$  being the comoving distance to the photon-decoupling epoch  $z_*$ . We use the Planck constraints for these parameters as provided in (Wang & Wang 2013).

For model I we solve the differential equation for  $h(z)$  appearing from Eq. (4), get  $w(z)$  and use it for further evaluation. Since by definition  $h(z=0) = 1$  we can solve for  $h(z)$  just by providing  $\Gamma/H_0$  and  $\Omega_{\text{m}}$  for a flat Universe. For model II and model III we solve equations (7) and (10) to obtain  $h(z)$  and the density parameters. Note that in these cases we keep the equation of state of the components of the Universe to be same as in the standard case. For model III we assume the dark energy is coupled to a radiation component and hence we use  $w_{\text{DR}}(z) = 1/3$  for dark radiation.

We work with three combinations of datasets: (i) We use the Union-2.1 compilation jointly with BAO data. (ii) Next we add  $H(2.34)$  to (i). (iii) Finally we include the values for the CMB shift parameters to SNIa, BAO and  $H(2.34)$  data. Note that for (i) and (ii) we use BBN constraints (Olive et al. 2014) of  $\Omega_{\text{b}}h^2$  as a prior.

We use CosmoMC (Lewis & Bridle 2002) to obtain a complete Markov Chain Monte Carlo (MCMC) estimation. Note that for model II and model III, there are certain non-physical areas in the parameter spaces<sup>7</sup>.

## 4 RESULTS

In order to gain a better understanding as to how our models might provide good fits to the observational data, we begin by showing results for concordance cosmology ( $\Lambda$ CDM). In figure 1 (left panel) we show the 1D marginalized likelihood of  $\Omega_{\text{m}}h^2$  obtained using different data combinations. In the right panel the 2D marginalized contours of  $\Omega_{\text{m}}$  vs  $H_0$  are shown. Constraints on different cosmological parameters are also given in table 1. We clearly see that the  $H(2.34)$  data point pushes the best-fit  $\Lambda$ CDM model towards a lower matter density as well as a lower Hubble parameter. Including the CMB (in combination with other data sets) pushes the best-fit back to a higher matter density and a higher Hubble parameter. This tension had earlier been reported in (Sahni et al. 2014; Delubac et al. 2015). One of the aims of the present analysis is to see whether one can alleviate this tension using our new DE models.

In figure 2 we show the results for Model I (exponentially decaying dark energy). In the top-left panel we plot the marginalized 1D likelihood of the decay parameter  $\Gamma/H_0$  obtained from different combinations of datasets. In the top-right panel we show the 1D marginalized likelihood for  $\Omega_{\text{m}}h^2$  while in the bottom-left panel we show the marginalized contour of  $\Omega_{\text{m}}$  vs  $H_0$  (these two plots can be compared with the corresponding results for  $\Lambda$ CDM shown in figure 1).

<sup>7</sup> We have not taken into account the most recent data (Alam et al. 2016) that was released when this paper was being prepared for publication. We expect our results and conclusions will not change considerably by incorporating these data.

In the bottom-right panel we show the marginalized contour of  $\{\Omega_{\text{DE}}, \Gamma/H_0\}$ . Our results indicate that the presence of the additional degree of freedom,  $\Gamma$ , increases the area of the confidence contours and reduces the tension between CMB data and the  $H(2.34)$  data point present in  $\Lambda$ CDM. However, the fact that the standard  $\Lambda$ CDM model lies close to the centre of the marginalized likelihood contours ( $\Gamma/H_0 = 0$ ) suggests that while Model I is viable, it is not strongly preferred over concordance cosmology.

From figure 2 we can see that both  $\Gamma > 0$  and  $\Gamma < 0$  are permitted by the data. As we mentioned earlier, a negative values of  $\Gamma$  imply an increase in the DE density with time which corresponds to phantom-like behaviour with  $w_{\text{eff}} < -1$ . In other words dark energy at late universe would have more density in comparison to the earlier times (at higher redshifts).  $\Gamma > 0$  implies decreasing in the DE density with time that can be effectively correspond to quintessence-like behaviour with  $w_{\text{eff}} > -1$ . We should also note that in both cases of  $\Gamma > 0$  and  $\Gamma < 0$ , the effective equation of state of dark energy cannot be a constant value and it would vary by time.

In figure 3 we show a few important quantities characterizing the expansion of the Universe. Top to bottom are shown: (a) the equation of state of dark energy  $w(z)$ , (b) the  $Om$  diagnostic,  $Om(z) = (h^2(z) - 1)/[(1+z)^3 - 1]$  (Sahni et al. 2008; Shafieloo et al. 2012), (c) the deceleration parameter  $q(z) = -\dot{H}/H^2 - 1$ . We plot 100 samples for these three quantities uniformly chosen from within the  $2\sigma$  range of the MCMC chains corresponding to different datasets. It is interesting that, for some parameter combinations, the slowing-down of cosmic acceleration appears to be consistent with the data.

In figures 4 and 5 we show our results for Model II (DE decaying into dark matter). Our results show that in this case there is no significant tension between the  $H(2.34)$  data point and CMB data. In fact Model II allows for a wide range of cosmological parameters to be consistent with the data. One should note that, unlike  $\Lambda$ CDM, there is a large overlap of confidence contours at the  $1\sigma$  level when plotted with and without CMB data. However, as in the case of Model I,  $\Lambda$ CDM lies close to the centre of the confidence contours, which is an indication of how well concordance cosmology is performing. From figure 4 we find that both  $\Gamma > 0$  and  $\Gamma < 0$  are permitted by the data.  $\Gamma > 0$  implies the transfer of energy from dark energy into dark matter, whereas  $\Gamma < 0$  implies the reverse. This transfer of energy results in the effective equation of state of DE being phantom-like ( $w_{\text{eff}} < -1$ ) for  $\Gamma < 0$  and quintessence-like ( $w_{\text{eff}} > -1$ ) for  $\Gamma > 0$ . Note that in both cases DE has the EOS of the cosmological constant, namely  $w = -1$ . However, the fact that the density of  $\Lambda$  is growing/decreasing at the expense of that of matter leads to either  $w_{\text{eff}} < -1$  when  $\rho_{\text{DM}} \rightarrow \rho_{\Lambda}$  ( $\Gamma < 0$ ) or to  $w_{\text{eff}} > -1$  when  $\rho_{\Lambda} \rightarrow \rho_{\text{DM}}$  ( $\Gamma > 0$ ).

Figures 6 and 7 show results for Model III (DE decaying into dark radiation). This model has a particular characteristic which precludes large flexibility if one considers high redshift data (such as CMB). In fact observational constraints set stringent limits on the amount of radiation density in the past. This is due to the fact that the radiation density increases by  $(1+z)^4$ , consequently its inferred value at high redshifts can change considerably if we change its current density by pumping energy from it into DE or vice versa.

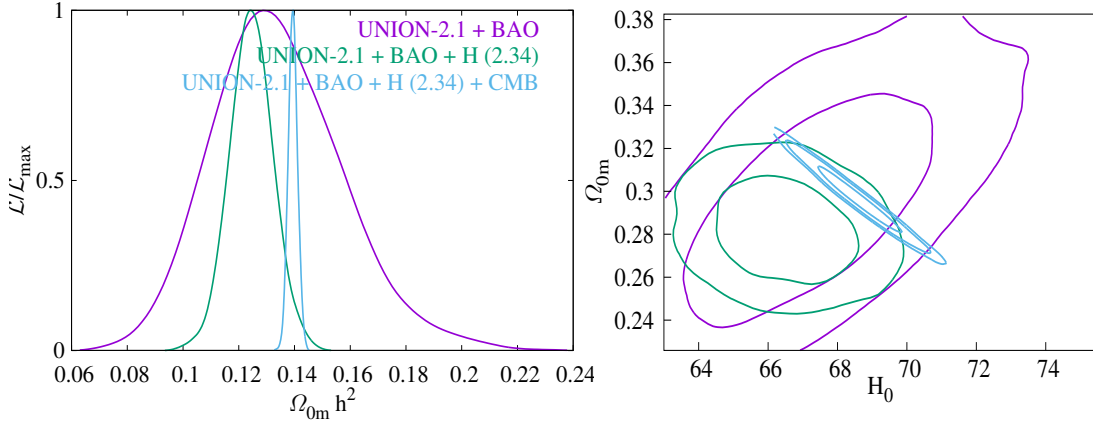


**Figure 1.** Observational constraints on standard  $\Lambda$ CDM. [Left] One dimensional marginalized likelihoods of  $\Omega_{0m}h^2$ . [Right]  $\{\Omega_{0m}, H_0\}$  contours for different datasets. The color-code convention for the right panel is identical to the left.

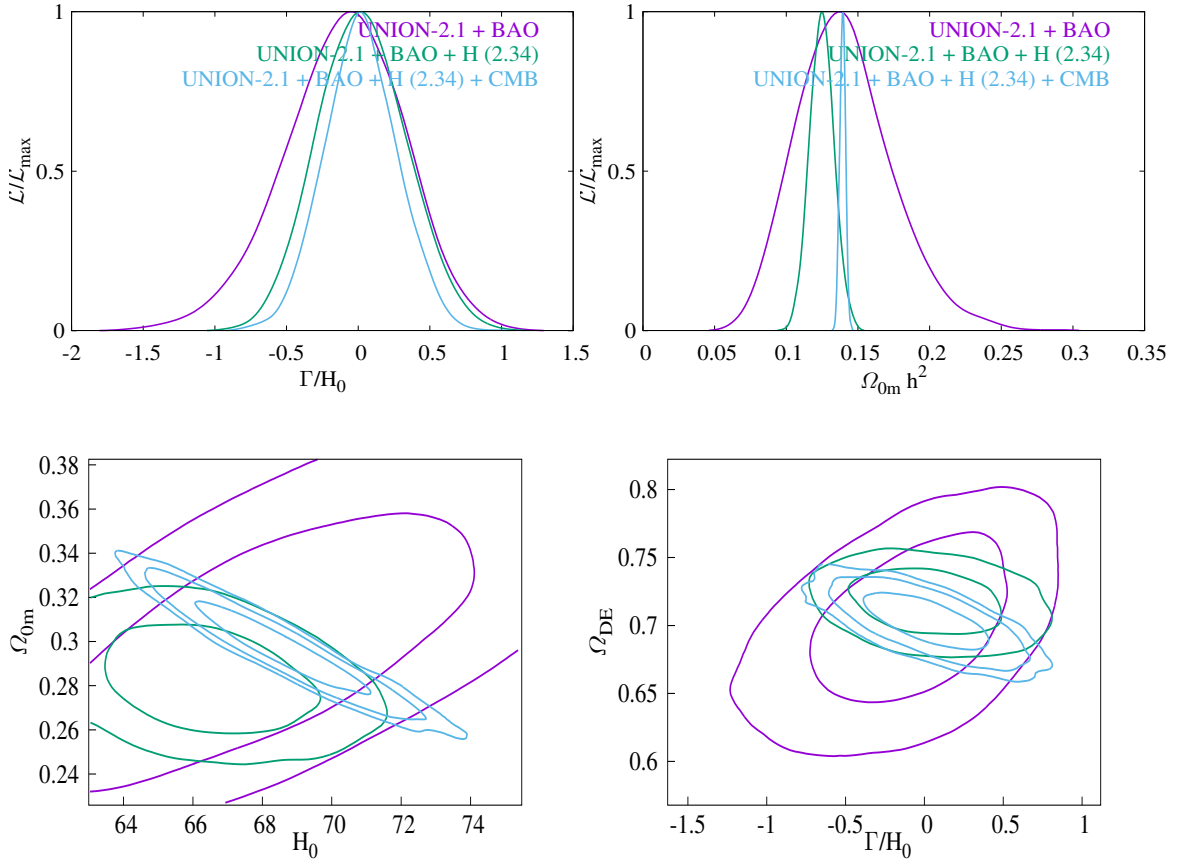


**Figure 2.** Results for Model I. [Top left] One dimensional marginalized likelihoods of the decay parameter in Eq. 2. [Top right] 1D likelihoods of  $\Omega_{0m}h^2$ . [Bottom left] 2D contours of  $\{\Omega_{0m}, H_0\}$ . [Bottom right] 2D contours of  $\{\Omega_{DE}, \Gamma/H_0\}$ . One can see that the tension between CMB data and the  $H(2.34)$  data point is somewhat reduced in this model.

Confronted with the data, Model III show a tiny possibility that dark energy might decay to dark radiation in small amounts. Our results also show that in this model one cannot alleviate the tension between the  $H(2.34)$  data point and CMB data. So in this sense model III resembles  $\Lambda$ CDM. This

model also posed us with some technical difficulties to derive the expansion history for different points in its parameter space due to divergence of some quantities.

In table 2 we show the derived values of the cosmological parameters for all three models. It is interesting that for

Model I and II the data permits a greater flexibility in the selection of cosmological parameters than  $\Lambda$ CDM. Also in these models, and especially in Model II, the tension between CMB and the  $H(2.34)$  data point is absent.

## 5 DISCUSSION

In this paper we propose a new class of dark energy models in which dark energy can decay, either exponentially in time, or into dark matter or into dark radiation with a time-independent rate. One might note that decaying DE models have been earlier discussed in the context of dark matter-dark energy interactions (Amendola 2000; Guo et al. 2007; Boehmer et al. 2008; Valiviita et al. 2008; He & Wang 2008; Micheletti et al. 2009; He et al. 2011; Pavan et al. 2012; Faraoni et al. 2014; Salvatelli et al. 2014; Ferreira et al. 2017), modified gravity (Sahni & Shtanov 2003; Shtanov et al. 2009) and quintessence (Gu & Hwang 2006; Alam et al. 2003; Kallosh et al. 2003; Blais & Polarski 2004; Wang et al. 2004; Dutta & Scherrer 2008; Gupta et al. 2012; Bolotin et al. 2012). The specialty of our model is that the decay of DE is related to the intrinsic properties of DE and not to the expansion of the Universe. Thus the properties of DE do not depend upon cosmological expansion or on the presence of a specific form of the DE potential or even on the equations governing cosmological expansion (viz. FRW, modified gravity, etc).

In a certain sense our class of models have much in common with the radioactive decay of matter. In similar fashion, one can describe the decay of DE in terms of a fundamental constant,  $\Gamma$ , which is related to the ‘half-life’ of DE as  $t_{1/2} = \ln(2)/\Gamma$ . The three models which we consider, though similar in equations and mechanism, give rise to somewhat different observational predictions. Model I describes dark energy decaying exponentially and as a result it has an evolving effective equation of state. Such models can be viable for a large region in parameter space and can *marginally* alleviate the tension between CMB and QSO based  $H(2.34)$  BAO data which is faced by  $\Lambda$ CDM.

In Model II, dark energy decays into dark matter. In this model the axis of confidence contours (derived from confronting the model with different sets of cosmological data) is rotated with respect to the case of Model I. Interestingly, data analysis using Model II shows absolutely no tension between any two sets of cosmology data. Indeed, the derived confidence contours all show proper overlap with each other – see figure 4. Incorporating CMB data into the analysis we find that Model II peaks strongly around the cosmological constant, that sets strong limits on the half-life of dark energy, namely that it needs to be several times the age of the Universe.

In Model III dark energy decays into dark radiation (DR). Cosmological observations place tight constraints on this model, especially when  $\Gamma < 0$  which corresponds to DR decaying to DE and implies an increase in the radiation density at high redshift.

In figure 8 we plot the  $H(z)$  samples within the  $2\sigma$  confidence level for different models and for different dataset combination that includes the QSO BAO data. Top left plot show the  $\Lambda$ CDM model results where we find the samples for the dataset combination with and without CMB data have

no overlap. Top right plot and bottom left plot show  $H(z)$  for model-I and model-II respectively. Note that both these models have substantial overlap of samples for Union-2.1 + BAO +  $H(2.34)$  and Union-2.1 + BAO +  $H(2.34)$  + CMB dataset combinations, suggesting no particular tension between CMB and QSO data. However as has been pointed out earlier, model-III does not help in alleviating the tension and the samples do not show consistency (unlike model-I and II).

To summarize, model II – in which DE decays to dark matter, is perhaps the most compelling of the three models which have been studied. All the three data sets which we consider, namely SNIa, BAO and CMB show consistency with each other for this fiducial cosmology and the  $2\sigma$  upper limit on  $|\Gamma|/H_0$  is less than 0.041 if all data are taken into account. Thus, since  $H_0 t_0 \sim 1$  for the best-fit  $\Lambda$ CDM model, this means that the half-life time for this channel of DE decay  $t_{1/2} > 17t_0 \approx 7 \times 10^{18}$  s where  $t_0$  is the present age of the Universe! For the other two models, some tension exists, especially between the CMB and the Lyman- $\alpha$  derived BAO at  $z = 2.34$ . Due to this tension, the obtained  $2\sigma$  limits on  $|\Gamma|/H_0$  for these channels of decay are not so strong as in the previous case. Still they both are significantly less than unity.

## ACKNOWLEDGMENTS

A.S. would like to acknowledge the support of the National Research Foundation of Korea (NRF-2016R1C1B2016478). DKH acknowledges Laboratoire APC-PCCP, Université Paris Diderot and Sorbonne Paris Cité (DXCACHEXGS) and also the financial support of the UnivEarthS Labex program at Sorbonne Paris Cité (ANR-10-LABX-0023 and ANR-11-IDEX-0005-02). A.A.S. was partially supported by the grant RFBR 17-02-01008 and by the Scientific Program P-7 of the Presidium of the Russian Academy of Sciences.

## REFERENCES

- Alam U., Sahni V., Starobinsky A. A., 2003, *JCAP*, 0304, 002  
 Alam S., et al., 2016, Submitted to: *Mon. Not. Roy. Astron. Soc.*  
 Amendola L., 2000, *Phys. Rev.*, D62, 043511  
 Anderson L., et al., 2013, *Mon. Not. Roy. Astron. Soc.*, 427, 3435  
 Beutler F., et al., 2011, *Mon. Not. Roy. Astron. Soc.*, 416, 3017  
 Blais D., Polarski D., 2004, *Phys. Rev.*, D70, 084008  
 Boehmer C. G., Caldera-Cabral G., Lazkoz R., Maartens R., 2008, *Phys. Rev.*, D78, 023505  
 Bolotin Yu. L., Lemets O. A., Yerokhin D. A., 2012, *Usp. Fiz. Nauk*, 182, 941  
 Boyarsky A., Ruchayskiy O., Iakubovskiy D., Franse J., 2014, *Phys. Rev. Lett.*, 113, 251301  
 Bronstein M., 1933, *Physikalische Zeitschrift der Sowietunion*, 3, 73  
 Carroll S. M., 2001, *Living Rev. Rel.*, 4, 1  
 Copeland E. J., Sami M., Tsujikawa S., 2006, *Int. J. Mod. Phys.*, D15, 1753  
 Delubac T., et al., 2015, *Astron. Astrophys.*, 574, A59  
 Dutta S., Scherrer R. J., 2008, *Phys. Rev.*, D78, 123525  
 Faraoni V., Dent J. B., Saridakis E. N., 2014, *Phys. Rev.*, D90, 063510  
 Ferreira E. G. M., Quintin J., Costa A. A., Abdalla E., Wang B., 2017, *Phys. Rev.*, D95, 043520  
 Gu J.-A., Hwang W.-Y. P., 2006, *Phys. Rev.*, D73, 023519

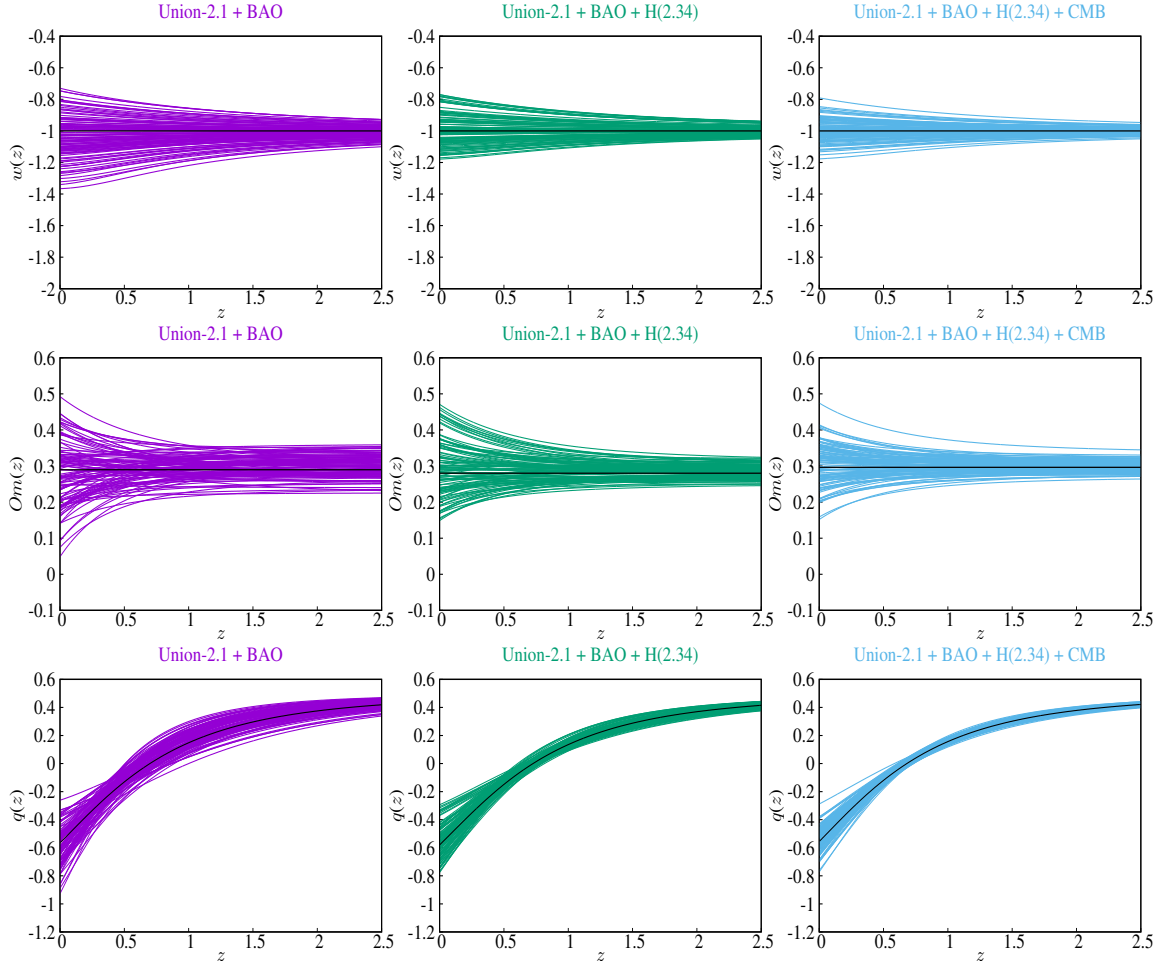


**Figure 3.** The equation of state of dark energy,  $w(z)$ , the  $Om$  diagnostic  $Om(z)$ , and the deceleration parameter  $q(z)$  (top, middle, bottom) are shown as a function of redshift for model I (Eq. 2). Left to right we plot samples within  $2\sigma$  CL's obtained from MCMC chains corresponding to Union-2.1 + BAO, Union-2.1 + BAO + H(2.34) and Union-2.1 + BAO + H(2.34) + CMB respectively. The black lines correspond to the best fit  $\Lambda$ CDM for the same combination of datasets.

Data	Union-2.1 + BAO	Union-2.1 + BAO + H (2.34)	Union-2.1 + BAO + H (2.34) + CMB
$\Omega_{\text{CDM}}h^2$	0.1071 $0.1119 \pm 0.026$	0.1017 $0.1023^{+0.0075}_{-0.0077}$	0.1166 $0.1166 \pm 0.0017$
$\Omega_{\text{m}}h^2$	0.129 $0.134^{+0.02}_{-0.026}$	0.124 $0.124^{+0.008}_{-0.007}$	0.139 $0.1394 \pm 0.0016$
$\Omega_{\text{m}}$	0.29 $0.294^{+0.033}_{-0.037}$	0.28 $0.282^{+0.015}_{-0.017}$	0.296 $0.297 \pm 0.01$
$H_0$	66.78 $67.27^{+2.13}_{-2.6}$	66.48 $66.48 \pm 1.3$	68.59 $68.6^{+0.77}_{-0.8}$
$-2 \ln \mathcal{L}_{\text{max}}$	546.1	546.2	550.25

**Table 1.** Best fit  $\chi^2_{\text{best fit}}$  and cosmological parameters obtained for different datasets for  $\Lambda$ CDM model. The best fit values (first row in each parameter) and the mean with  $1\sigma$  deviations (second row in each parameter) are also provided for some parameters.

Guo Z.-K., Ohta N., Tsujikawa S., 2007, *Phys. Rev.*, D76, 023508

Gupta G., Majumdar S., Sen A. A., 2012, *Mon. Not. Roy. Astron. Soc.*, 420, 1309

He J.-H., Wang B., 2008, *JCAP*, 0806, 010

He J.-H., Wang B., Abdalla E., 2011, *Phys. Rev.*, D83, 063515

Kallosh R., Kratochvil J., Linde A. D., Linder E. V., Shmakova M., 2003, *JCAP*, 0310, 015

Lewis A., Bridle S., 2002, *Phys. Rev.*, D66, 103511

Lima J. A. S., Basilakos S., Sola J., 2013, *Mon. Not. Roy. Astron. Soc.*, 431, 923

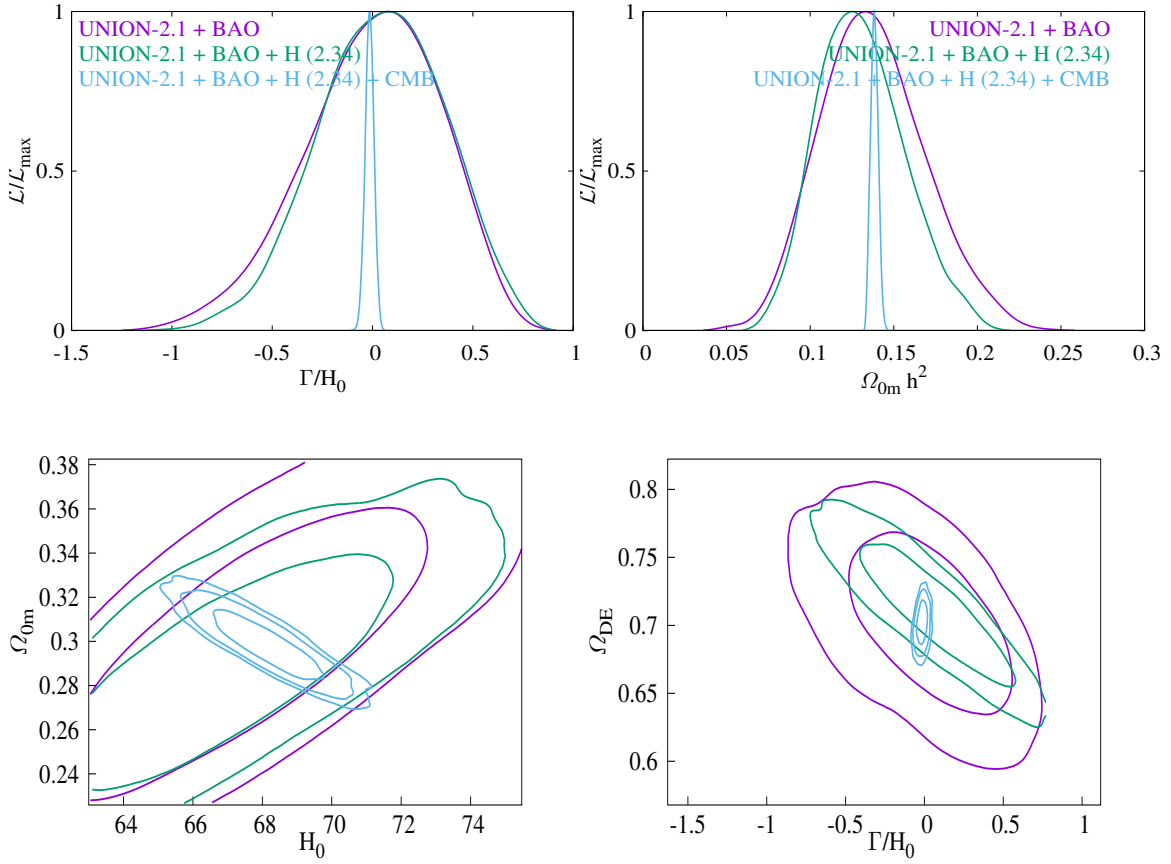


**Figure 4.** Results for Model II. [Top left] One dimensional marginalized likelihoods of the decay parameter  $\Gamma$  are shown for model II (Eq. 7). [Top right] 1D likelihoods of  $\Omega_{\text{m}} h^2$ . [Bottom left] 2D contours of  $\{\Omega_{\text{m}}, H_0\}$ . [Bottom right] 2D contours of  $\{\Omega_{\text{DE}}, \Gamma/H_0\}$ . Unlike  $\Lambda$ CDM, no tension between CMB data and the  $H(2.34)$  data point is indicated for Model II.

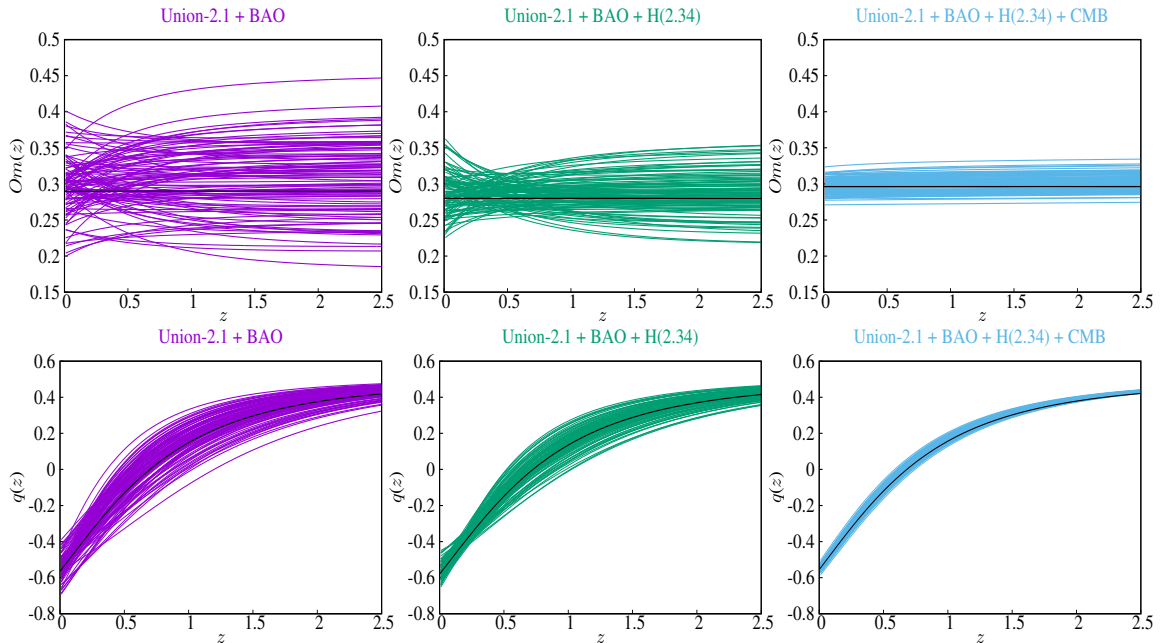


**Figure 5.** Samples of  $Om(z)$  and  $q(z)$  for model II (Eq. 7). The datasets are indicated at the top of each plot. The black lines correspond to the best fit  $\Lambda$ CDM for the same combination of datasets.



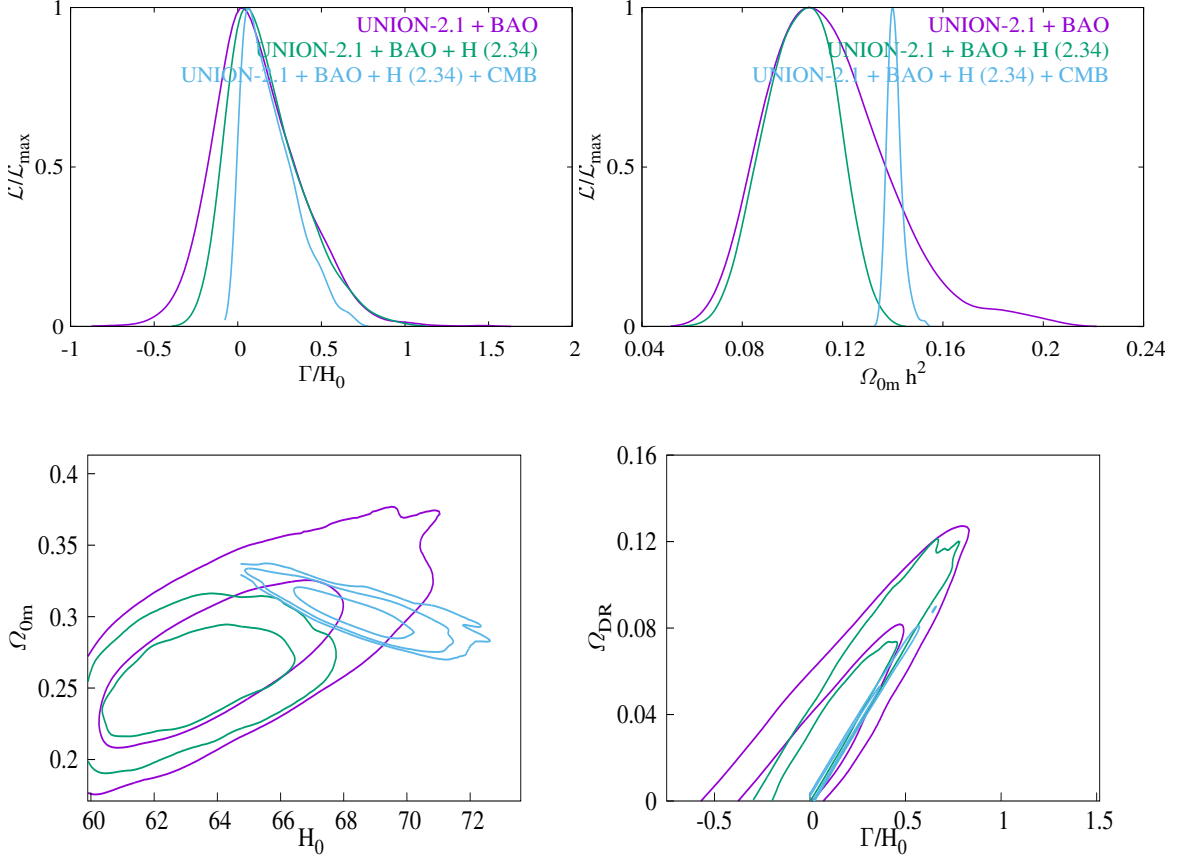


**Figure 6.** Results for Model III. [Top left] One dimensional marginalized likelihoods of the decay parameter  $\Gamma$  for model III (Eq. 10). [Top right] 1D likelihoods of  $\Omega_m h^2$ . [Bottom left] 2D contours of  $\{\Omega_m, H_0\}$ . [Bottom right] 2D contours of  $\{\Omega_{Dr}, \Gamma/H_0\}$ . Model III seems to fail in alleviating the tension between the datasets since radiation density is tightly constrained.

Data	Union-2.1 + BAO			Union-2.1 + BAO + H (2.34)			Union-2.1 + BAO + H (2.34) + CMB		
	Model I	Model II	Model III	Model I	Model II	Model III	Model I	Model II	Model III
$\Omega_{CDM} h^2$	0.111 0.119 <sup>+0.027</sup> <sub>-0.038</sub>	0.113 0.115 <sup>+0.028</sup> <sub>-0.035</sub>	0.104 0.093 <sup>+0.018</sup> <sub>-0.028</sub>	0.102 0.103 ± 0.008	0.116 0.109 <sup>+0.022</sup> <sub>-0.03</sub>	0.1 0.081 <sup>+0.015</sup> <sub>-0.014</sub>	0.116 0.116 ± 0.002	0.116 0.116 ± 0.002	0.117 0.119 <sup>+0.002</sup> <sub>-0.004</sub>
$\Omega_m h^2$	0.133 0.141 <sup>+0.027</sup> <sub>-0.038</sub>	0.135 0.137 <sup>+0.028</sup> <sub>-0.035</sub>	0.126 0.114 <sup>+0.018</sup> <sub>-0.028</sub>	0.124 0.123 <sup>+0.01</sup> <sub>-0.007</sub>	0.138 0.13 <sup>+0.022</sup> <sub>-0.03</sub>	0.122 0.103 <sup>+0.015</sup> <sub>-0.014</sub>	0.139 0.139 ± 0.002	0.138 0.138 ± 0.002	0.139 0.14 <sup>+0.002</sup> <sub>-0.004</sub>
$\Omega_{dr} h^2$	-	-	0 0.016 <sup>+0.018</sup> <sub>&lt;</sub>	-	-	0.01 0.017 <sup>+0.006</sup> <sub>&lt;</sub>	-	-	0 0.013 <sup>+0.005</sup> <sub>&lt;</sub>
$\Omega_m$	0.292 0.3 <sup>+0.038</sup> <sub>-0.04</sub>	0.296 0.298 ± 0.04	0.284 0.28 <sup>+0.03</sup> <sub>-0.04</sub>	0.282 0.283 <sup>+0.015</sup> <sub>-0.017</sub>	0.298 0.28 ± 0.03	0.282 0.26 <sup>+0.028</sup> <sub>-0.024</sub>	0.298 0.297 ± 0.013	0.297 0.299 ± 0.01	0.298 0.3 ± 0.01
$\Omega_{dr}$	-	-	0 0.04 <sup>+0.01</sup> <sub>&lt;</sub>	-	-	0.02 0.04 <sup>+0.01</sup> <sub>&lt;</sub>	-	-	0 0.03 <sup>+0.008</sup> <sub>&lt;</sub>
$H_0$	67.52 68.12 <sup>+3.9</sup> <sub>-4.5</sub>	67.6 67.5 ± 3.4	66.8 64.4 <sup>+2</sup> <sub>-3.1</sub>	66.26 66.4 ± 1.9	68 67 <sup>+2.8</sup> <sub>-3.5</sub>	66 63.4 <sup>+1.75</sup> <sub>-2.04</sub>	68.34 68.5 ± 1.6	68.2 68.1 <sup>+1</sup> <sub>-1.1</sub>	68.5 68.5 ± 1.2
$\Gamma/H_0$	-0.085 -0.1 <sup>+0.45</sup> <sub>-0.38</sub>	0.13 0 <sup>+0.39</sup> <sub>-0.28</sub>	-0.12 0.12 <sup>+0.2</sup> <sub>-0.3</sub>	0.03 0.028 ± 0.3	0.16 0.04 <sup>+0.34</sup> <sub>-0.3</sub>	0.13 0.17 <sup>+0.14</sup> <sub>-0.27</sub>	0.046 0.02 ± 0.25	-0.011 -0.015 ± 0.02	0.005 0.2 <sup>+0.05</sup> <sub>-0.19</sub>
-2 ln $\mathcal{L}_{max}$	546.1	546	546.1	546.2	546	546.2	550.2	550	550.2

**Table 2.** Best fit  $\chi^2_{best\ fit}$  obtained for different models considering different combination of datasets. The best fit values of cosmological parameters is shown in the first row, and the mean (with 1 $\sigma$  deviations) is shown in the second row. P.C. refers to the situation where the posterior distribution is cut in the prior range. A ‘<’ symbol denotes that the parameter is unbounded from below.

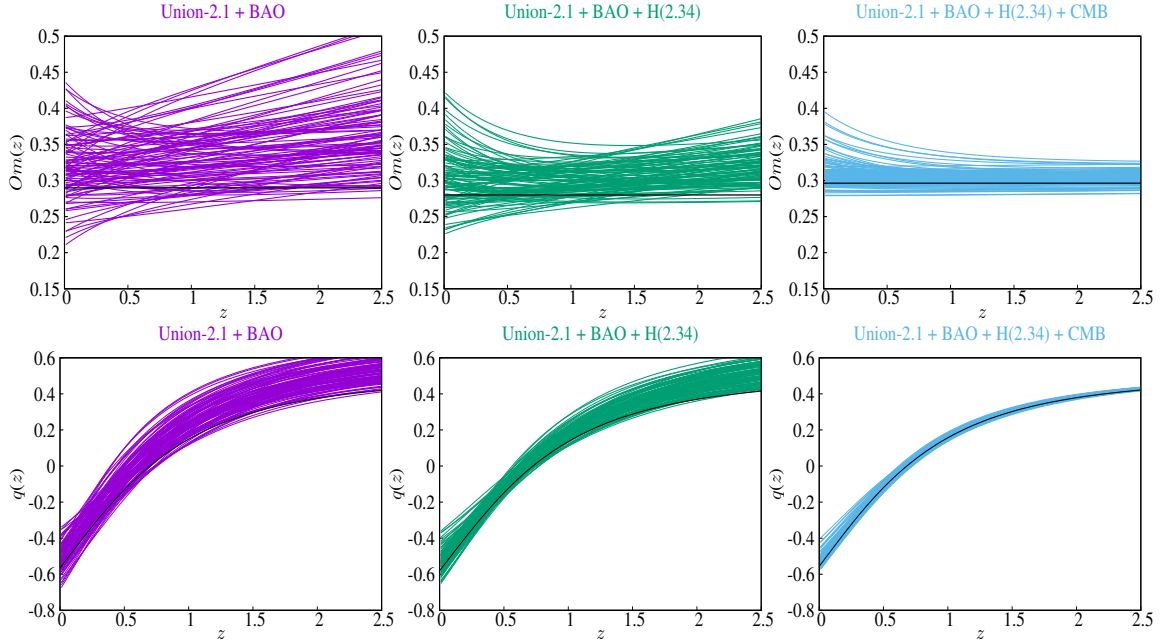


**Figure 7.** Samples  $Om(z)$  and  $q(z)$  as a function of redshift for model-III (Eq. 10). The datasets are indicated at the top of each plot. The black lines correspond to the best fit  $\Lambda$ CDM, for the same combination of datasets.

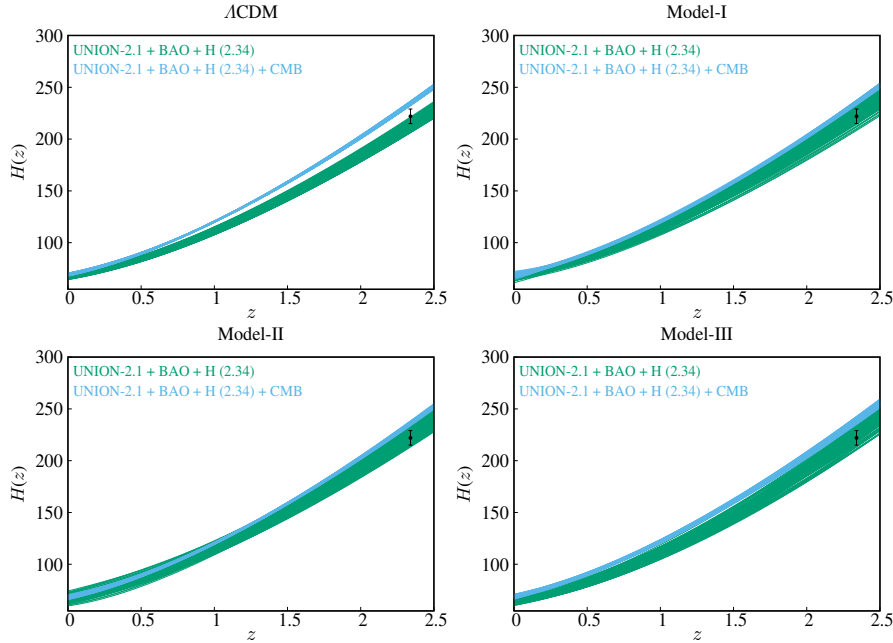


**Figure 8.** Samples  $H(z)$  as a function of redshift for different models are provided for 2 different dataset combination that include  $H(z = 2.34)$  measurement. The datasets are indicated at the top of each plot. Note that we have 100 samples in each case representing the allowed region within  $2\sigma$ . We find that for model-I and model-II there are large overlap between the samples while for  $\Lambda$ CDM and model-III, the samples show discordance, especially in the former case. The QSO BAO data is plotted in black with errorbar.

Micheletti S., Abdalla E., Wang B., 2009, *Phys. Rev.*, D79, 123506  
 Olive K. A., et al., 2014, *Chin. Phys.*, C38, 090001  
 Ozer M., Taha M. O., 1986, *Phys. Lett.*, B171, 363  
 Padmanabhan T., 2003, *Phys. Rept.*, 380, 235  
 Pavan A. B., Ferreira E. G. M., Micheletti S., de Souza J. C. C.,  
 Abdalla E., 2012, *Phys. Rev.*, D86, 103521  
 Peebles P. J. E., Ratra B., 2003, *Rev. Mod. Phys.*, 75, 559

Percival W. J., et al., 2010, *Mon. Not. Roy. Astron. Soc.*, 401,  
 2148  
 Sahni V., 2004, *Lect. Notes Phys.*, 653, 141  
 Sahni V., 2005, in *Proceedings, 14th Workshop on General Relativity and Gravitation (JGRG14): Kyoto, Japan, November 29-December 3, 2004*. pp 95–115 ([arXiv:astro-ph/0502032](https://arxiv.org/abs/astro-ph/0502032))  
 Sahni V., Shtanov Y., 2003, *JCAP*, 0311, 014

- Sahni V., Starobinsky A. A., 2000, *Int. J. Mod. Phys.*, D9, 373  
Sahni V., Starobinsky A., 2006, *Int. J. Mod. Phys.*, D15, 2105  
Sahni V., Shafieloo A., Starobinsky A. A., 2008, *Phys. Rev.*, D78, 103502  
Sahni V., Shafieloo A., Starobinsky A. A., 2014, *Astrophys. J.*, 793, L40  
Salvatelli V., Said N., Bruni M., Melchiorri A., Wands D., 2014, *Phys. Rev. Lett.*, 113, 181301  
Shafieloo A., Sahni V., Starobinsky A. A., 2012, *Phys. Rev.*, D86, 103527  
Shapiro I. L., Sola J., 2002, *JHEP*, 02, 006  
Shtanov Y., Sahni V., Shafieloo A., Toporensky A., 2009, *JCAP*, 0904, 023  
Suzuki N., et al., 2012, *Astrophys. J.*, 746, 85  
Valiviita J., Majerotto E., Maartens R., 2008, *JCAP*, 0807, 020  
Wang Y., Wang S., 2013, *Phys. Rev.*, D88, 043522  
Wang Y., Kratochvil J. M., Linde A. D., Shmakova M., 2004, *JCAP*, 0412, 006  
Wang B., Abdalla E., Atrio-Barandela F., Pavon D., 2016, *Rept. Prog. Phys.*, 79, 096901

## APPENDIX A: $H^2(z)$ IN THE LARGE DECAY TIME LIMIT

Though to determine the evolution law  $h^2(z)$  we have solved Eqs. (2.3), (2.4-2.6) and (2.7-2.9) exactly, to understand the answers it is instructive to consider the limit of large decay times  $|\Gamma| \ll H_0$  which is both expected and follows from our calculations. Then it becomes possible to present explicit expressions for  $h^2(z)$ .

### A1 Model I

For  $\Gamma t \ll 1$ , we get in the first order:

$$\rho_{DE} = \epsilon_0 e^{-\Gamma t} \approx \epsilon_0(1 - \Gamma t) \quad (\text{A1})$$

$$h^2(z) = \Omega_{0m}(1+z)^3 + (1 - \Omega_{0m})[1 - \Gamma(t - t_0)] \quad (\text{A2})$$

Here the  $t(z)$  dependence in the last term can taken from the  $\Lambda$ CDM model with the same value of  $\Omega_{0m}$ :

$$t(z) = t_0 - H_0^{-1} \int_0^z \frac{dz_1}{1+z_1} \left[ 1 - \Omega_{0m} + \Omega_{0m}(1+z_1)^3 \right]^{-1/2} \quad (\text{A3})$$

Thus, with the same accuracy:

$$h^2(z) = 1 - \Omega_{0m} + \Omega_{0m}(1+z)^3 + \frac{\Gamma(1 - \Omega_{0m})}{H_0} \int_0^z \frac{dz_1}{1+z_1} \left[ 1 - \Omega_{0m} + \Omega_{0m}(1+z_1)^3 \right]^{-1/2} \quad (\text{A4})$$

It is clearly seen that  $h^2(z)$  in this model is always *larger* in the past compared to the standard  $\Lambda$ CDM model with the same value of  $\Omega_{0m}$ .

Let us now compare this result with what happens in the case of DE being slowly rolling quintessence,

i.e. a scalar field  $\phi$  with a potential  $V(\phi)$  minimally coupled to gravity. The assumption  $\Gamma t_0 \ll 1$  means that the change in  $V(\phi)$  is small up to the present time  $t_0$ . So, we can expand  $V(\phi) = V_0 + V_{\phi 0}\psi$  where  $\psi = \phi - \phi_0$ ,  $\phi_0 = \phi(t_0)$ ,  $V_0 = V(\phi_0)$ ,  $V_{\phi 0} = \frac{dV}{d\phi}(\phi_0)$ . Then

$$\psi = V_{\phi} \int_t^{t_0} \frac{dt_1}{a^3(t_1)} \int_0^{t_1} a^3(t_2) dt_2, \quad \rho_{DE} = V_0 + V_{\phi 0}\psi + \frac{\dot{\psi}^2}{2}$$

$$h^2 = \Omega_m(1+z)^3 + (1 - \Omega_m) \left[ 1 + \frac{V_{\phi 0}^2}{V_0} \int_t^{t_0} \frac{dt_1}{a^3(t_1)} \int_0^{t_1} a^3(t_2) dt_2 + \frac{V_{\phi 0}^2}{2a^6 V_0} \left( \int_0^t a^3(t_1) dt_1 \right)^2 \right] \quad (\text{A5})$$

Once more, the  $t(z)$  dependence in all integrals is taken from the  $\Lambda$ CDM model with the same value of  $\Omega_m$ . Though Eq. (A5) is slightly more complicated than Eq. (A4), consideration of the future de Sitter stage with  $H_{dS} = H_0 \sqrt{1 - \Omega_m}$  (that occurs as far as  $\Gamma t \ll 1$ ) shows that here

$$\Gamma = \frac{V_{\phi 0}^2}{3H_{dS} V_0} \quad (\text{A6})$$

**A2 Model II & III**

In the same approximation:

---

$$\begin{aligned}
\dot{\rho}_{DE} &= -\Gamma\rho_{DE} \\
\Gamma &= \text{const} \\
\dot{\rho}_m + 3H\rho_m &= \Gamma\rho_{DE} \\
\rho_{DE} &\approx \epsilon_0(1 - \Gamma t), \quad \rho_m \approx \frac{\text{const}}{a^3} + \Gamma\epsilon_0 \int_0^t a^3 dt \\
h^2(z) &= 1 - \Omega_{0m} + \Omega_{0m}(1+z)^3 + \Gamma \left[ t_0 - t(z) - a^{-3} \int_t^{t_0} a^3(t_1) dt_1 \right] \\
&= 1 - \Omega_{0m} + \Omega_{0m}(1+z)^3 - \frac{\Gamma(1 - \Omega_{0m})}{H_0} \int_0^z \frac{dz_1}{1+z_1} \left[ 1 - \Omega_{0m} + \Omega_{0m}(1+z_1)^3 \right]^{-1/2} \left[ \left( \frac{1+z}{1+z_1} \right)^3 - 1 \right] \quad (\text{A7})
\end{aligned}$$


---

Here, we find just the opposite,  $h^2(z)$  is *smaller* in the past compared to the standard case. This crucial difference between the models is due to different equations of state of products of DE decay in them and because of their normalization to the present relative amount of dark matter  $\Omega_{0m}$ . It is straightforward to generalize this result to the model

III with DE decay into dark radiation. In this case the situation appears to be the same as for the model I:  $h^2(z)$  was relatively larger in the past.

This paper has been typeset from a  $\text{\TeX}/\text{\LaTeX}$  file prepared by the author.